J. Mol. Model. **1996**, *2*, 319 – 326

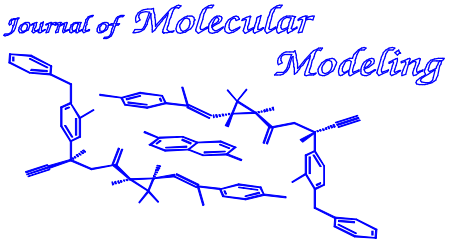

Gibbs-Ensemble Molecular Dynamics: A New Method for Simulations Involving Particle Exchange

Reinhard Hentschke*, Tim Bast, Ewald Aydt, and Michael Kotelyanskii

Max-Planck-Institut für Polymerforschung, Postfach 3148, D - 55021 Mainz, Germany
(hentschk@mpip-mainz.mpg.de)

Received: 15 May 1996 / Accepted: 6 August 1996 / Published: 27 September 1996

Abstract

We discuss a novel simulation method suitable for simulating phenomena involving particle exchange. The method is a molecular dynamics version of the Gibbs-Ensemble Monte Carlo technique, which has been developed some years ago for the direct simulation of phase equilibria in fluid systems. The idea is to have two separate simulation boxes, which can exchange particles or molecules in a thermodynamically consistent fashion. We discuss the general idea of the Gibbs-Ensemble Molecular Dynamics technique and present examples for different simple atomic and molecular fluids. Specifically we will discuss Gibbs-Ensemble Molecular Dynamics simulations of gas-liquid and liquid-solid equilibria in Lennard-Jones systems and in hexane as well as an application of the method to adsorption.

Keywords: Gibbs-Ensemble MD, Monte Carlo, particle exchange, adsorption

Introduction

There are numerous phenomena, which can be studied via computer simulation, where it is advantageous or even necessary to vary the particle number during the simulation. Three simple examples may serve to illustrate this point. The forces between two planar surfaces at close proximity can be related to the microscopic interactions on the molecular scale using the so called surface force apparatus [1]. A computer simulation of a surface force apparatus would have to include not only the solid surface-to-solid surface interface. Usually there are molecules adsorbed or tethered to the surfaces as well as the molecules of a liquid filling the intermediate space. In addition there has to be a reservoir, where those liquid molecules can be 'deposited', which are squeezed out from between the surfaces as the inter-surface separation is reduced. Thus, such simulations are plagued by the comparatively large portion of the system devoted to the 'interface' between the slit and the reservoir, which causes unwanted artifacts. A second example is the simulation of osmotic phenomena. Here the computer simulation would have to include both the osmotic cell as well as the corresponding bulk solvent surrounding it. One may for instance think of simulating the swelling of a polymer network in contact with a solvent. Because molecular simulations still contain rarely more than a few thousand atoms, the inclusion of a large interfacial region may render such a simulation impossible (for realistic systems). Finally, we may think about the adsorption equilibrium between a porous bulk solid (e.g., zeolites) and a gas. Here the comparatively small external surface area of the solid contributes little to the overall adsorbing surface area and even may be ill de-

* *To whom correspondence should be addressed*

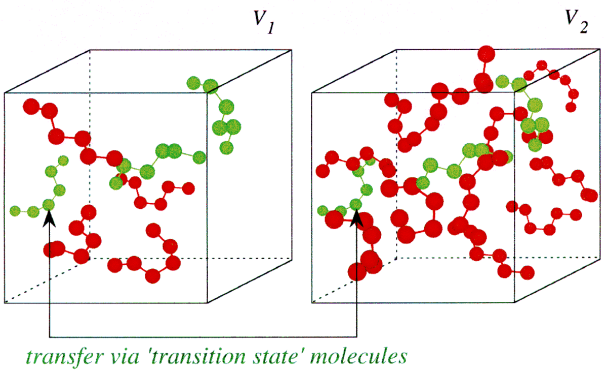

Figure 1. *Sketch of two simulation volumes or boxes with the respective volumes V_1 and V_2 exchanging molecules.*

fined. Again one faces a situation, where in principle it is sufficient to model a small number of unit cells of the porous bulk solid in which gas particles are inserted or eliminated according to the chemical potential of the surrounding gas. Thus, these examples illustrate the motivation for simulating open systems in which the number of molecules is no longer constant.

In the 1970's the Monte Carlo methodology was extended to include such open systems through the development of the grand canonical Monte Carlo (GCMC) method [2–4]. An extension of the Molecular Dynamics method to open systems (GCMD) was not developed until about 20 years later [5, 6]. However, in most applications a certain deficiency of both the GCMC and GCMD methods is the need for specifying or independently calculating the chemical potential. Even though the latter in principle can be determined, based on the Widom potential-distribution theory [7, 8], from NVT Monte Carlo [9] or Molecular Dynamics [10, 11], this adds another complicated calculation. A method which combines these two aspects into a single simulation run was developed by Panagiotopoulos [12] in the context of phase coexistence in one-component fluids. The Gibbs-Ensemble Monte Carlo (GEMC) technique does not require the reference chemical potential as input. In GEMC two separate simulation volumes can exchange particles or molecules so that in equilibrium, for instance, the temperature, the pressure and the chemical potential in the boxes are the same (cf. figure 1). In this fashion a single simulation run of a one-component fluid at a particular subcritical temperature and pressure yields the pure gas and the pure liquid at coexistence, where each one occupies its respective simulation volume. However, other thermodynamic conditions, for instance requiring different pressures in the two simulation volumes, are also easy to implement [13]. A drawback of the MC based methods usually is the low acceptance rate for particle creation or insertion in a dense phase. That Molecular Dynamics may be better suited for dense systems was first suggested by Cagin [14], who also discusses the idea of a Molecular Dynamics version of the Gibbs-Ensemble method. Shortly afterwards the GEMD method was indeed realized via two independent approaches [15–17].

It is one of these approaches, i.e., [16, 17], on which we focus in the following. First we discuss the general idea as well as the specific implementation of the method. We then illustrate its performance using a number of examples, i.e., the gas-liquid-solid phase behavior of Lennard-Jones systems as well as the gas-liquid phase behavior of a realistic molecular system, which here is n-hexane. Finally, we show an application of the method to adsorption in a zeolite, which pertains to the last of the examples discussed above.

The GEMD method

The GEMC method originally was introduced in [12] to simulate the liquid-gas coexistence of a single-component fluid system. In this case one has two physically separated volumes or simulation boxes, whose combined volume and combined particle number is constant (as a consequence of the phase rule). Both boxes are at the same temperature and pressure. In addition they can exchange particles in a way such that the chemical potential also is the same in both boxes. For a specified temperature, and with the proper choice of the total volume, the system may phase separate so that there will be the pure liquid in one box and the pure coexisting gas in the other. This can happen below the critical temperature, when the average density corresponds to the thermodynamically unstable states below the liquid-vapor coexistence line. In the following we discuss an analogous scheme for a molecular system within the MD framework.

The potential

In conventional MD one numerically solves the equations of motion for a system of N particles contained in a box of volume V having the total potential energy U. Here we consider a molecular system consisting of N atoms in M molecules, and we write the total potential energy U as a sum over inter- and intra-molecular interactions, i.e.

$$U = U_{inter} + U_{intra} = \sum_{\substack{i<j \\ \alpha\in i,\beta\in j}} \Phi\left(\vec{r}_{\alpha\beta}\right) + \sum_i U_{intra}\left(\{\vec{r}_{\alpha\in i}\}\right) \qquad (1)$$

The first term, U_{inter}, is the sum over atom-atom pair potentials $\Phi\left(\vec{r}_{\alpha\beta}\right)$, where $\vec{r}_{\alpha\beta} = \vec{r}_\alpha - \vec{r}_\beta$, and $\vec{r}_a$ and $\vec{r}_\beta$ are the position vectors of the atoms labeled α and β be-

longing to two different molecules *i* and *j*. The second potential energy term, U_{intra}, encompasses all interactions within a molecule, i.e., bond stretching, valence angle and torsional distortions as well as intra-molecular non-bonded interactions.

In order to simulate a variable number of molecules in each of the two boxes we introduce an additional degree of freedom ξ_i for every molecule *i*. ξ_i can vary between 1 and 0, where ξ_i=1 means that the molecule *i* is in box 1, whereas ξ_i=0 means that it is in box 2. For 1> ξ_i > 0 the molecule is in a 'transition state', where it is 'felt' in both boxes. Thus, we rewrite the inter-molecular potential energy of the system as a function of the coordinates and the ξ_i as

$$\begin{aligned} &U_{inter}\left(\{\vec{r}_\alpha\},\{\xi_i\},V_1,V_2\right) = \\ &\sum_{\substack{i<j \\ \alpha\in i,\beta\in j}} \left[\Phi\left(\vec{r}_{\alpha\beta},V_1\right)\xi_i\xi_j + \right. \\ &\left. + \Phi\left(\vec{r}_{\alpha\beta},V_2\right)\left(1-\xi_i\right)\left(1-\xi_j\right)\right] + \sum_i g\left(\xi_i\right) \\ &= U_1 + U_2 + \sum_i g\left(\xi_i\right) \end{aligned} \tag{2}$$

where V_1 and V_2 are the volumes of the two boxes. The first two terms, U_1 and U_2, represent the inter-molecular potential energies of the first and the second box, respectively. Notice that as soon as we apply periodic boundary conditions and the inter-particle interactions are calculated involving the particle's closest images, the distance between them, and therefore the inter-molecular potential energy, is a function of the box dimensions (or the volume if the shape of the box is kept fixed).

At equilibrium the number of unphysical but necessary transition state molecules should be small in comparison to the total number of molecules. What exactly 'small' means we will define below. However, to satisfy this condition it often is necessary to introduce an additional potential function g(ξ_i) > 0, which is equal to zero only at ξ_i=0 and at ξ_i=1. Here we use

$$g\left(\xi_i\right) = \begin{cases} \omega\left[\tanh\left(u\xi_i\right) + \tanh\left(u\left(1-\xi_i\right)\right) - 1\right] & , \quad 0 \le \xi_i \le 1 \\ \infty & , \quad otherwise \end{cases} \tag{3}$$

This additional potential introduces a barrier of height w and steepness u between the states corresponding to the 'real' particles or molecules, i.e., particles or molecules which are entirely in one or the other of the two boxes, making the transition state unfavorable.

The GEMD equations of motion

In the following we present the equations of motion for our GEMD method. In the case of liquid gas-coexistence in a one-component system the temperature, the pressure, and the chemical potential, even though the latter two are not explicitly specified, must be equal in the two phases and thus in the two boxes. Similar to the GEMC method this can be achieved if every change of the volume of one of the boxes is accompanied by an opposite but equal change of the volume of the other box. Thus, the total volume of the two boxes is constant, while the individual volumes are variable. The GEMD equations of motion describing this case are

$$\begin{aligned} \dot{\vec{r}}_\alpha &= m_\alpha \dot{\vec{r}}_\alpha \\ \dot{\vec{p}}_\alpha &= -\frac{\partial U}{\partial \vec{r}_\alpha} - \eta\,\vec{p}_\alpha \\ \dot{\eta} &= \frac{1}{Q_T}\left[\sum_\alpha \frac{\vec{p}_\alpha^{\,2}}{m_\alpha} - Xk_BT\right] \\ p_{\xi_i} &= m_{\xi_i}\dot{\xi}_i \end{aligned} \tag{4}$$

$$\begin{aligned} \dot{p}_{\xi_i} &= -\frac{\partial U}{\partial \xi_i} = \\ &= -\sum_{\substack{i(\neq j) \\ \alpha\in i,\beta\in j}} \left[\Phi\left(\vec{r}_{\alpha\beta},V_1\right)\xi_j - \Phi\left(\vec{r}_{\alpha\beta},V_2\right)\left(1-\xi_j\right)\right] - \sum_i \frac{\partial}{\partial\xi_i} g\left(\xi_i\right) \\ p_{V_1} &= Q_P \dot{V}_1 \\ \dot{p}_{V_1} &= P_1^e - P_2^e \end{aligned}$$

Here $\vec{p}_\alpha$ and p_{ξ_i} are the momenta conjugate to the cartesian coordinates $\vec{r}_\alpha$ and the transfer coordinate x_i, respectively. h is an additional degree of freedom, and Q_T is a parameter governing the temperature relaxation. The first three equations describe the evolution of a system coupled to an external heat bath with the temperature *T* [18], where *X* is a coefficient, which is equal to the number of degrees of freedom coupled to the thermostat. If there would be only one box, this would correspond to the well known NVT simulation algorithm, with the temperature being controlled via a Nose-Hoover thermostat. The next two equations govern the evolution of the x_i, i.e., the transfer of the molecules between the boxes. The last two equations are the equations of motion of the box volume V_1, where p_{V_1} is a momentum variable conjugate to V_1, and Q_P is a parameter governing the volume relaxation. Thus, the volume changes are controlled by the difference between the instantaneous values of the 'external' pressures P_1^e and P_2^e in the two boxes. Here, for each box, we employ the (sin-

gle-box) constant-pressure MD algorithm proposed in reference [19], i.e., if again there would be only one box, say the first box, the equations $p_{V_1} = Q_P \dot{V}_1$ and $\dot{p}_{V_1} = P_1^e - P$ would be identical to the equations of motion derived for the box volume in reference [19] (cf. also equation (16) in reference [20]), where P is just the preassigned pressure, which here is replaced by the instantaneous external pressure P_2^e in the second box. Here

$$P_1^e = \sum_{\substack{i>j \\ \alpha\in i,\beta\in j}} \frac{1}{3V_1}\left(\vec{\nabla}_{\vec{r}_{\alpha\beta}} \Phi\left(\vec{r}_{\alpha\beta}, V_1\right)\xi_i \xi_j \vec{R}_{1,n}\right) \tag{5}$$

where $\vec{R}_{1,n} = V_1^{1/3}\left(n_x, n_y n_z\right)$ is a vector, which maps the separation of the coordinates $\vec{r}_\alpha$ and $\vec{r}_\beta$ into the proper distance between the atoms α and β according to the minimum image convention assuming a cubic box. In this algorithm the $\vec{r}_\alpha$ are not scaled by the box dimensions and they are not mapped back into the box according to the boundary conditions whenever a particle leaves the primary box and enters one of the surrounding image boxes. The coupling to the volume fluctuations rather happens through the positions of the image particles. Note that the summations involving the inter-particle or inter-molecular interactions in the equations (1), (2), (4), and (5) are meant to implicitly include the interactions between the primary particles or molecules with their (nearest) images. Thus some care has to be taken in the case of the interaction of a particle or molecule with it's own images. Note also that a detailed discussion including a formal justification of the above equations of motion is given in [16, 17].

The above equations of motion are appropriate for the simulation of two-phase coexistence in a one-component system, and we will discuss two examples below. In order to simulate two-phase coexistence in a two-component system, the last two equations in (4) are replaced by

$$\begin{aligned} p_{V_k} &= Q_P \dot{V}_k \\ \dot{p}_{V_k} &= P_k^e - P \end{aligned} \tag{6}$$

where k = 1,2. The GEMD equations of motion appropriate for the examples discussed in the introduction are even more simple. In these cases the last two equations in (4) are replaced by

$$\begin{aligned} p_{V_1} &= Q_p \dot{V}_1 \\ \dot{p}_{V_1} &= P_1^e - P \end{aligned} \tag{7}$$

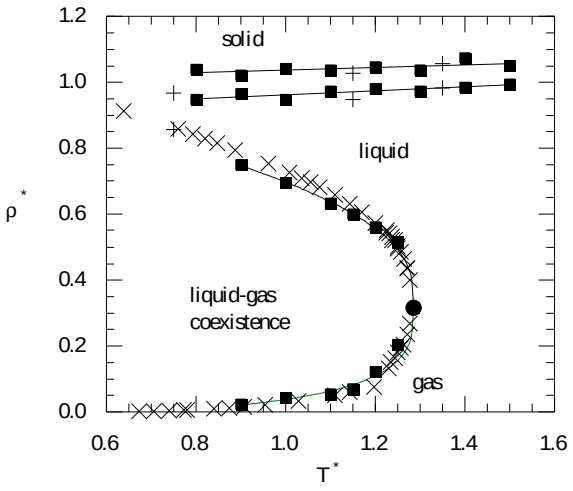

Figure 2. *Phase diagram of the Lennard-Jones system in terms of the LJ density, ρ*, and the LJ temperature, T*. The solid squares indicate the GEMD results for the location of the phase boundaries. The solid lines are fits to the GEMD results as explained in the text. The crosses and the plusses are experimental data points for methane and argon, respectively.*

Here P is the pressure in the reference system represented by box 2, i.e., the pressure in the liquid outside the force apparatus or in the reference solution in contact with the swollen network or the pressure of the gas in contact with the porous solid.

Some technical aspects

If a long-range cutoff distance r_{cut} is used when calculating the non-bonded interactions, then the corresponding continuum corrections modify $\dot{p}_{\xi_i} = -\partial U / \partial \xi_i$ in equation (4), where we must add $-\partial\left(U_1^{cor} + U_2^{cor}\right)\Big/\partial\xi_i$ to the right hand side. In the case of Lennard-Jones non-bonded interactions, the usual long-range corrections become

$$U_1^{cor} \approx \sum_{\nu\mu} \frac{1}{2} 4\pi \frac{1}{V_1} \sum_i \xi_i \sum_j \xi_j \int_{r_{cut}}^{\infty} \Phi_{\nu\mu}(r) r^2 dr \tag{8}$$

and U_2^{cor} is given by an analogous expression in which ξ_i is replaced by $(1 - \xi_i)$ and V_1 is replaced by V_2. The indexes ν and μ in equation (8) label distinct atom types in the interacting molecules i and j. The only other change affects P_k^e (where k = 1,2). Here we must add the correction

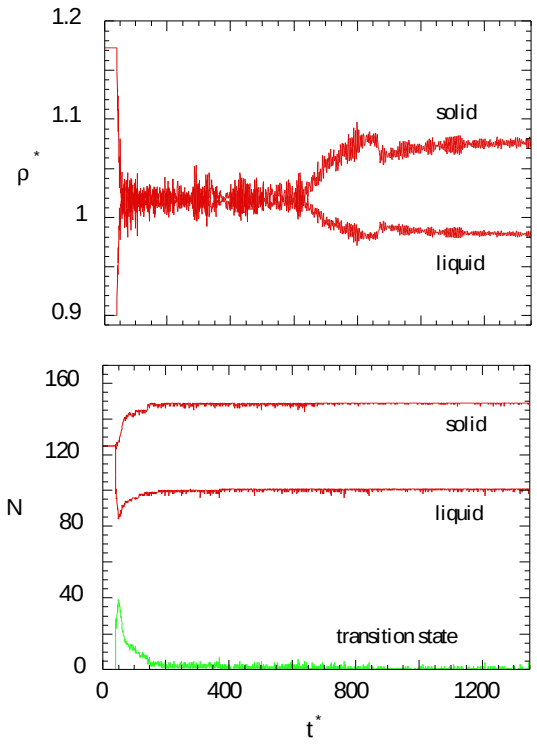

Figure 3. *The upper panel shows the time evolution of ρ* for the two boxes at T*=1.4 in the case of liquid-solid coexistence. The lower panel shows the corresponding evolution of the number of particles N in the solid (upper curve), in the liquid (middle curve) and in the transition state (bottom curve).*

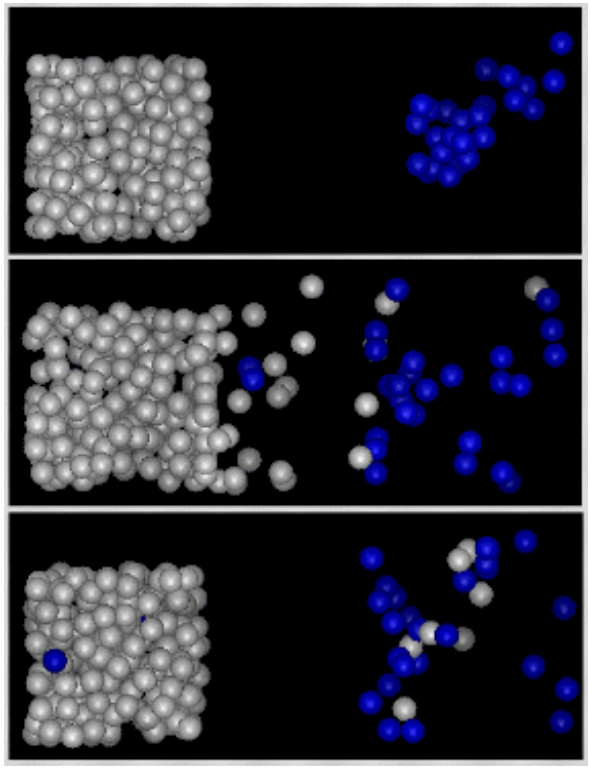

Figure 4. *The three panels illustrate the particle exchange between the two boxes for one temperature at different times towards the beginning as well as towards the end of the simulation run. Here the ξ_i-values of the transition state particles are used to scale their cartesian position relative to the shifted positions of the boxes, which in reality are superimposed. The color coding distinguishes particles, which initially are in different boxes (top). Subsequently the transfer is allowed. Early on there are more particles in the transfer state (middle) than at later times (bottom)*

$$P_1^{e,cor} \approx -\sum_{\nu\mu} \frac{2\pi}{3} \frac{1}{V_1^2} \sum_i \xi_i \sum_j \xi_j \int_{r_{cut}}^{\infty} \frac{d\Phi_{\nu\mu}(r)}{dr} r^3 dr \qquad (9)$$

where $P_2^{e,cor}$ is also given by (9), however, again with the above replacements for ξ_i and V_1.

The GEMD method discussed here also requires a short-range cutoff r'_{cut}. This is because two atoms α and β belonging to the respective molecules i and j may 'collide' due to the strong divergence of $\Phi(\vec{r}_{\alpha\beta})$ as $\vec{r}_{\alpha\beta} \to 0$ even though according to their ξ-values, i.e., $\xi_i \approx 0$ and $\xi_j \approx 1$, they would belong to different boxes. Thus, the value for r'_{cut} should meet two requirements. It should be sufficiently large to minimize the effect of unphysical ghost collisions. In addition it should not affect the interactions between atoms belonging to the same box. In the Lennard-Jones systems described below, the optimal value for r'_{cut} can be found via a series of independent NVT simulations (in the relevant temperature and density range) using increasing values for r'_{cut}. The best value for r'_{cut} lies just below the onset of noticeable effects on the average pressure and other bulk properties. In the following examples we use r'_{cut} = 0.88 (in Lennard-Jones units). It should be noted that currently we assume a constant non-bonded potential below the short-range or 'ghost' cutoff distance. However, other functional forms, which approach a finite value at $\vec{r}_{\alpha\beta} = 0$, are possibly better alternatives.

The equations of motion (4) do not depend on explicit threshold ξ_i-values according to which a particle is counted as being in box 1, in box 2, or in the transition state. Nevertheless the transition state is an artificial state, whose population should be small in comparison to the population of the real states represented by the particles considered to belong to either of the two boxes. In other words, for long times each particle should be either 'close to 0' or 'close to 1' most of the time. 'Close' means that the long time deviation of the particle's ξ_i-values from 0 or 1 has a negligible effect on the bulk properties of the systems rep-

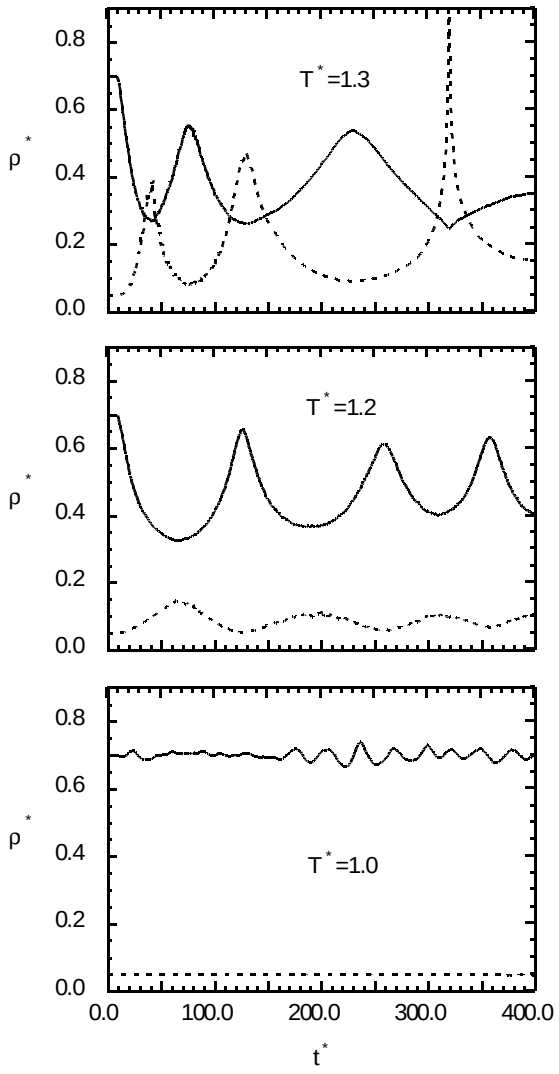

Figure 5. *This series of panels each shows the evolution of the densities (gas: dashed line; liquid: solid line) at different temperatures below and close to the critical point for the case of gas-liquid coexistence in the LJ system. Note that the spike-like feature in the upper panel is due to a numerical constraint on the maximum fluctuation of the volume.*

resented by the two boxes. That this is indeed the case is illustrated by the examples below. However, for bookkeeping purposes, we sometimes distinguish between particles belonging to box 1 or to the transition state or to box 2 according to whether their ξ_i-values are in the range between 1 and $1 - 10^{-4}$ or between $1 - 10^{-4}$ and 10^{-4} or between 10^{-4} and 0. It should be noted in this context that we use the Verlet algorithm to integrate the equations of motion. A special modification, described in detail in reference [17], can be used to handle the 'hard walls' at 0 and 1 along the ξ_i-direction.

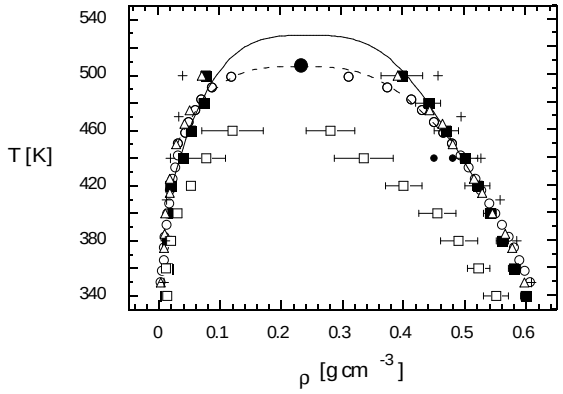

Figure 6. *Liquid-gas coexistence curve for hexane. Hollow circles: experimental data; hollow triangles: GEMC result obtained with a 13.8 Å cutoff including long-range corrections. The large solid circle corresponds to the experimental critical point. Hollow squares: GEMD using a cut and shifted LJ potential, were the long-range cutoff is at 10 Å; solid squares: using a 15 Å cut-off instead; small solid circles (at T=440 K): liquid densities for a 12 Å and a 14 Å cutoff, respectively; plusses: result obtained for a 10 Å cutoff including long-range corrections. The error bars indicate standard deviations. These are omitted for the plusses in order to not obscure the figure. The lines (solid: GEMD; dashed: experiment) are again fits as described in the text to figure 2.*

Finally we like to mention that the stability of the numerical solution of (4) is markedly improved if the Berendsen thermostat [21] is used instead of the Nose-Hoover thermostat. Even though only for the latter one can mathematically justify that the algorithm does produce the proper ensemble averages, the obtained results were the same in both cases within the statistical error [17]. An additional numerical improvement of the algorithm can be achived by also thermalizing the transfer degrees of freedom by a direct coupling to the Berendsen thermostat. This and some related aspects are discussed in detail in [22].

Application to phase coexistence in Lennard-Jones and molecular systems

Our first application is the gas-liquid-solid phase diagram of the Lennard-Jones (LJ) system, using the inter-particle potential $4\varepsilon[(\sigma/r)^{12} - (\sigma/r)^6]$ including long-range continuum corrections [22]. The GEMD density-temperature phase diagram is shown in figure 2. The solid boundary of the gas-liquid coexistence density is a fit based on the law of rectilinear diameters, $(\rho_l + \rho_g)/2 = \rho_c + C_1 (1 - T/T_c)^\beta$, together with the power law $\rho_l - \rho_g = 2C_2 (1 - T/T_c)^\beta$ using the

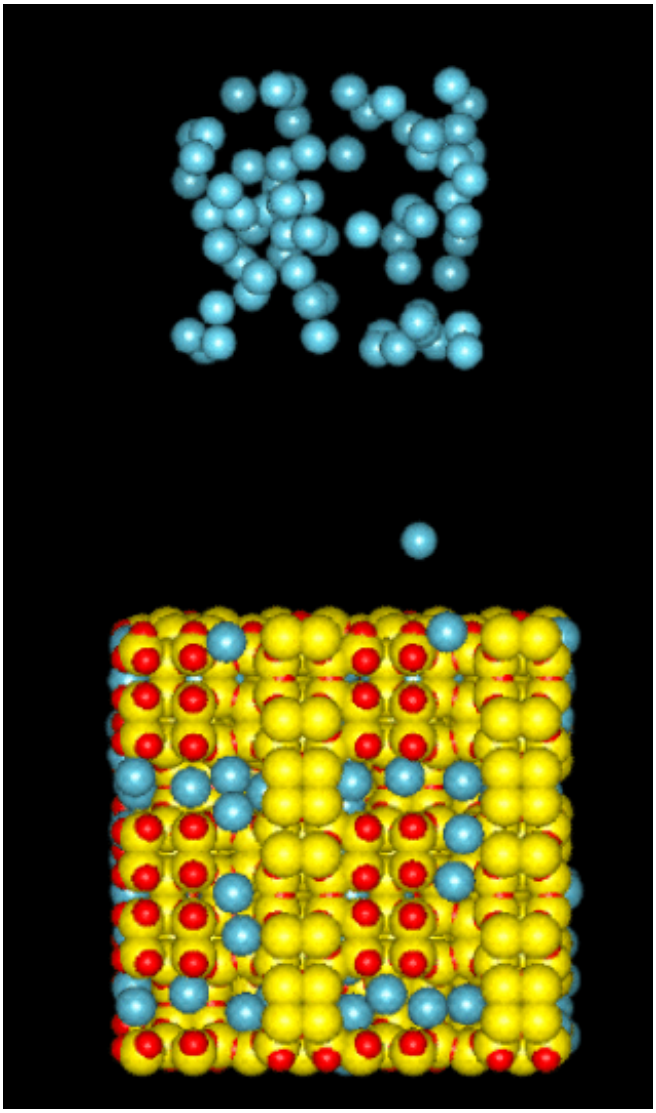

Figure 7. *Using an analogous representation as in figure 4 this figure shows a snapshot of the model zeolite (bottom) containing methane molecules (shown as blue spheres) diffusing along channels in the zeolite. The methane molecules can transfer between the gas phase (top) and the cavities in the solid.*

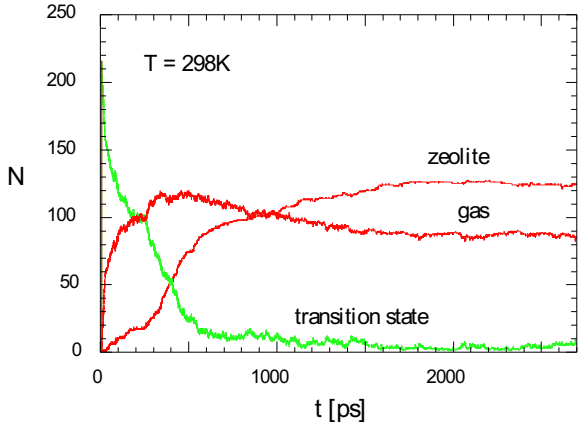

Figure 8. *Time evolution of the number of particles N in the zeolite, in the gas box, and in the transition state.*

critical density, ρ_c, the critical temperature, T_c, and C_1 as well as C_2 as fit parameters. For β we use the 3D Ising value of ≈ 0.325. The experimental data for methane, shown for comparison, are taken from [23]. The data are converted to LJ units via $\varepsilon/k_B = 148.7$ K and $\sigma = 3.79$Å based on a fit to the experimental 2nd virial coefficient. Figure 2 also includes the liquid-solid coexistence, showing that the GEMD method works well at high densities. Here the solid lines are simply least-squares fits to the GEMD results. The experimental data are for argon, again using the LJ parameters obtained via the 2nd virial coefficient to convert to LJ units [24]. The scatter of the GEMD results in this case is due to the rather small system containing a total of 250 particles. The deviation of the simulation data from the experimental results near the triple point is possibly due to the oversimplified form of the potential (cf. [24] and a reference therein). Figure 3 shows the evolution of the particle density for the case of liquid-solid coexistence together with the corresponding instantaneous particle numbers corresponding to the liquid, the solid, and the transition state. Notice that the number of particles in the transition state quickly decreases to a level which is low compared to the number of particles in the boxes. The three snapshots shown in figure 4, which correspond to one particular temperature ($k_BT/\varepsilon = 1.0$), present a pictorial illustration of the particle transfer at different times along the system's trajectory. Figure 5, finally, shows the gas-liquid density evolution for a series of temperatures below and close to the critical temperature. Notice how the densities in the two boxes become virtually indistinguishable near the critical temperature as they should.

We also want to include the analogous phase diagram for gas-liquid coexistence in a molecular system. Figure 6 shows the corresponding result for hexane in a system containing a total of 144 molecules. The details of the model potential and the specific parameters used in this calculation are described elsewhere [17]. The agreement between GEMD and GEMC [25, 26] as well as with the experiment [27] is quite good, depending of course on the accuracy of the interaction potential. Notice that the position of the coexistence region in the T-ρ-plane is quite sensitive to the choice of r_{cut} and the inclusion of long-range corrections.

Application to adsorption

Here we briefly want to mention some preliminary results obtained for the physisorption of methane in a zeolite using the GEMD approach. For the sake of comparison we

chose silicalite I (ZSM5), which has been studied via GCMC by Goodbody et al. [28]. In this case the atoms of the solid do not transfer between the boxes, one of which contains eight ZSM5 unit cells and the other corresponds to the gas phase. Again the details of the model parameters will be given elsewhere [29].

Figure 7 shows a simulation snapshot, which illustrates the methane transfer between the gas phase and the cavities in the solid. The actual evolution of the number of particles in the two boxes as a function of time is shown in figure 8 at a gas pressure of 70 bar and a temperature of 298 K. Notice that the gas box is kept at constant pressure, whereas the zeolite box is kept at constant volume. This situation therefore corresponds to the set of equations of motion, where the last two equations in (4) are replaced by the equations (7).

Conclusion

The above examples show that the GEMD method is useful for simulations in which a single large molecular system can be replaced by two smaller systems, which exchange molecules at constant chemical potential. The specific advantage of the two-box approach is that the chemical potential in the reference system must not be determined separately. An advantage that the GEMD method has over the GEMC method is that it provides direct dynamic information in the two boxes, like the self-diffusion coefficient in the two coexisting phases [17]. Another important point is that the GEMD method performs quite well in dense systems.

References

1. Israelachvili, J. *Intermolecular and Surface Forces*; Academic Press: London, 2nd ed., 1992.
2. Norman, G. E.; Filinov, V. S. *High Temp. Res. USSR* **1969**, *7*, 216.
3. Adams, D. *Mol. Phys.* **1974**, *28*, 1241-1252.
4. Adams, D. Mol. Phys. 1975, 29, 307-311.
5. Cagin, T.; Pettitt, B. M. *Mol. Simul.* **1991**, *6*, 5-26.
6. Cagin, T.; Pettitt, B. M. *Mol. Phys.* **1991**, *72*, 169-175.
7. Widom, B. *J. Chem. Phys.* **1963**, *39*, 2808-2812.
8. Widom, B. *J. Phys. Chem.* **1982**, *86*, 869-872.
9. Shing, K. S.; Gubbins, K. E. *Mol. Phys.* **1983**, *49*, 1121.
10. Romano, S.; Singer, K. *Mol. Phys.* **1979**, *37*, 1765-1772.
11. Powles, J. G.; Evans, W. A. B.; Quirke, N. *Mol. Phys.* **1982**, *46*, 1347-1370.
12. Panagiotopoulos, A. Z. *Mol. Phys.* **1987**, *61*, 813-826.
13. Panagiotopoulos, A. Z. *Mol. Simul.* **1992**, *9*, 1-23.
14. Cagin, T. In *Computer Aided Innovation of New Materials II*; Doyama, M., Kihara, J., Tanaka, M., Yamamoto, R., Eds.; Elsevier Science Publishers, 1993; pages 255-259.
15. Palmer, B. J.; Lo, C. *J. Chem. Phys.* **1994**, *101*, 10899-10907.
16. Kotelyanskii, M. J.; Hentschke, R. *Phys. Rev.* **1995**, *51*, 5116-5119.
17. Kotelyanskii, M. J.; Hentschke, R. *Mol. Simul.* **1996**, *17*, 95-112.
18. Hoover, W. G. *Phys. Rev.* **1985**, *31*, 1695-1697.
19. Winkler, R. G.; Morawitz, H.; Yoon, D. Y. *Mol. Phys.* **1992**, *75*, 669-688.
20. Winkler, R. G.; Hentschke, R. *J. Chem. Phys.* **1993**, *99*, 5405-5417.
21. Berendsen, H. J. C.; Postma, J. P. M.; van Gunsteren, W. F.; DiNola, A.; Haak, J. R. *J. Chem. Phys.* **1984**, *81*, 3684-3690.
22. Bast, T.; Kotelyanskii, M.; Hentschke, R. in preparation, 1996.
23. Grigor, A. F.; Steele, W. A. *J. Chem. Phys.* **1968**, *48*, 1032-1037.
24. Hansen, J.-P.; Verlet, L. *Phys. Rev.* **1969**, *184*, 151-161.
25. Siepmann, J. I.; Karaborni, S.; Smit, B. *Nature* **1993**, *365*, 330-332.
26. Computer simulations of vapour-liquid phase equilibria of n-alkanes. Smit, B.; Karaborni, S.; Siepmann, J. I. preprint, 1995.
27. Smith, B. D.; Srivastava, R. Thermodynamics Data for Pure Compounds: Hydrocarbons and Ketones; Elsevier: Amsterdam, 1986.
28. Goodbody, S. J.; Watanabe, K.; MacGowan, D.; Walton, J. P. R. B.; Quirke, N. *J. Chem. Soc. Faraday Trans.* **1991**, *87*, 1951-1958.
29. Aydt, E. M.; Bast, T.; Hentschke, R. in preparation, 1996.